tion of ethyl iodide increases along the abscissa of Fig. 3, the energy absorbed directly by C_2H_5I, the ratio $G(HI)/G(I_2)$, the G of radicals formed from n-C_5H_{12}, and the nature of the chemical environment of each reactive species are presumably all changing. The net sum of these effects yields the straight line relationship.

Conclusions.—The work reported here seems to require that the reaction $RI + e^- \rightarrow R + I^-$ occurs to a significant extent to explain the yield of R radicals from RI additives during the radiolysis of RI–pentane solutions. Figures 1 and 2 indicate that the concentration range of RX in which the R radical yield rises from low values to its saturation value is similar to the range suggested by Platzman[4] as the most probable for the competition of solutes for subexcitation electrons which would otherwise undergo recombination with positive ions. If electron attachment plays a significant role it must be that in these solutions the immediate recapture of electrons by the parent positive ion suggested by the estimates of Samuel and Magee[22] does not occur with high probability, or that the probability of the $e^- + RI \rightarrow R + I^-$ reaction is sufficiently high (requiring of the order of 10 collisions or less) that it can compete for the electron while it is making its round trip from the positive ion into the solution and back. Escape of the electrons from the parent positive ion is suggested by experiments of R. Ahrens[23] and B. Suryanarayana in our laboratory, in which the change in electrical conductivity of liquid ammonia caused by exposure to 10^{18} e.v. g.$^{-1}$ min.$^{-1}$ of Co^{60} gamma radiation was measured. These are consistent with the conclusion that the steady state concentration of ion pairs caused by the radiation field was 4×10^{12} cc.$^{-1}$.

The evidence of this paper and earlier work both suggest that radical production from irradiated hydrocarbons is reduced when neutralization of RH^+ ions occurs by charge transfer from negative ions, such as I^-, rather than by combination with free electrons. If this is so it means that radical yields for hydrocarbons deduced from iodine scavenger studies may be lower than the actual radical yields in the pure hydrocarbons.

Acknowledgment.—The work of this paper was supported in part by the United States Atomic Energy Commission under contract AT (11-1)-32 and in part by the University Research Committee with funds made available by the Wisconsin Alumni Research Foundation.

---

(22) A. H. Samuel and J. L. Magee, *J. Chem. Phys.*, **21**, 1080 (1953).

(23) R. Ahrens, Ph.D. Thesis, University of Wisconsin, 1959, available from University Microfilms, Ann Arbor, Michigan.

[CONTRIBUTION FROM UNION CARBIDE EUROPEAN RESEARCH ASSOCIATES, S.A., BRUSSELS, AND UNIVERSITY OF WISCONSIN, MADISON, WISCONSIN]

The Preparation, Properties and Structure of the Iron Carbonyl Carbide $Fe_5(CO)_{15}C$

BY EMILE H. BRAYE,[1] LAWRENCE F. DAHL,[2] WALTER HÜBEL[1] AND DALE L. WAMPLER[3]

RECEIVED MAY 5, 1962

The reaction of $Fe_3(CO)_{12}$ with methylphenylacetylene and in particular with pentyne-1 gives besides organometallic complexes a small quantity (*i.e.*, less than 0.5% yield in the most favorable cases) of a new type of polynuclear metal complex of formula $Fe_5(CO)_{15}C$. The conditions of preparation and properties of $Fe_5(CO)_{15}C$ are described. Magnetic and infrared spectral studies show the solid to be diamagnetic with no bridging carbonyl groups. Its molecular configuration was found by a three-dimensional X-ray analysis to consist of an approximate equilateral tetragonal pyramid of iron atoms with three terminal carbonyls attached to each iron. A new structural feature is the presence of a penta-coördinated carbon atom located slightly below the center of the basal plane of iron atoms at approximately equal distances from each of the five iron atoms. This carbon atom with its four valence electrons allows each iron to attain a "closed shell" electronic structure in the ground state. A qualitative MO description of the new type of bonding is given.

Introduction

The reactions of the three iron carbonyls with alkynes in inert solvents[4–10] have produced a variety of organoiron carbonyl complexes with unusual structural features and novel types of bonding. The present paper reports the preparation and characterization by both chemical and physical means of a new type of compound, a polynuclear metal carbonyl carbide, of formula $Fe_5(CO)_{15}C$.

This compound was isolated in small amounts during the investigation of the reactions between alkynes and triiron dodecacarbonyl.[4–6] In particular, formation of $Fe_5(CO)_{15}C$ was observed on heating $Fe_3(CO)_{12}$ with methylphenylacetylene or pentyne-1 in petroleum ether. The compound could only be obtained in 0.5% yield in the most favorable cases, and all attempts to increase the yield were unsuccessful. Elemental chemical analysis indicated an approximate $Fe(CO)_3$ species. The degree of polymerization in the crystalline state was established by a three-dimensional X-ray study reported here which not only showed the molecular

---

(1) Union Carbide European Research Associates, s.a., Brussels 18, Belgium.

(2) Department of Chemistry, University of Wisconsin, Madison 6, Wisconsin.

(3) National Science Foundation Predoctoral Research Fellow, 1959–1961. The X-ray work is abstracted in part from the Ph.D. Thesis of Dale L. Wampler, University of Wisconsin, January 1962.

(4) W. Hübel, E. H. Braye, A. Clauss, E. Wiess, U. Krüerke, D. A. Brown, G. S. D. King and C. Hoogzand, *J. Inorg. Nuclear Chem.*, **9**, 204 (1959).

(5) W. Hübel and E. H. Braye, *ibid.*, **10**, 250 (1959).

(6) E. H. Braye, C. Hoogzand, W. Hübel, U. Krüerke, R. Merényi and E. Weiss, "Advances in the Chemistry of the Coördination Compounds," edited by S. Kirschner, The Macmillan Co., New York, N. Y., 1961, pp. 190–198.

(7) G. N. Schrauzer, *J. Am. Chem. Soc.*, **81**, 5307 (1959).

(8) W. Hübel and E. Weiss, *Chem. and Ind.* (*London*), 703 (1959).

(9) E. Weiss, R. G. Merényi and W. Hübel, *ibid.*, 407 (1960).

(10) H. W. Sternberg, R. Markby and I. Wender, *J. Am. Chem. Soc.*, **80** 1009 (1958),

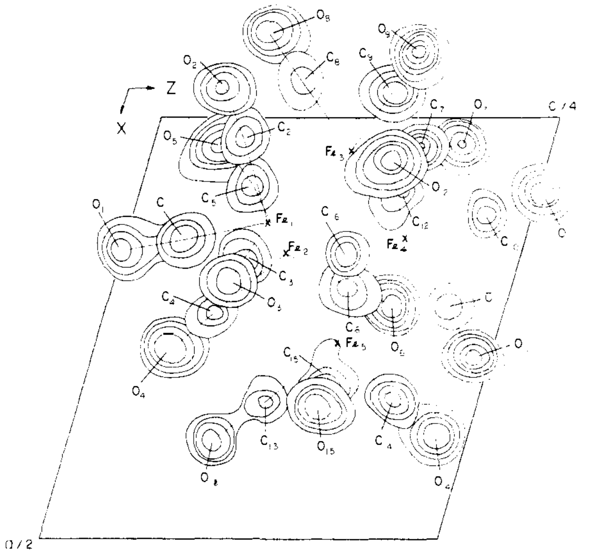

Fig. 1.—A composite of contour sections parallel to (010) of the final three-dimensional electron-density synthesis showing the carbon and oxygen atoms. The positions of the five iron atoms are marked. Contours are at intervals of 1 $e/\text{Å}.^3$ with lowest contour at 3 $e/\text{Å}.^3$.

configuration to be a pentamer but also revealed the existence of the extra carbon atom, subsequently verified by the chemical analysis.

Experimental

Preparation and Properties.—The conditions for the compound's formation were quite critical. A systematic variation of the reaction parameters in the case of pentyne-1 never gave a yield above *ca.* 0.5% by weight, based on $Fe_3(CO)_{12}$. Iron dodecacarbonyl (25 g., 50 mmoles), pentyne-1 (4.9 ml., 52 mmoles) and 220 ml. petroleum ether were heated in a 0.5 l. autoclave with stirring for 5–6 hours at 90°. The filtered reaction mixture was evaporated to dryness *in vacuo* in order to remove the $Fe(CO)_5$ formed. The precipitate and the residue were taken up in warm petroleum ether (about 500 ml.) and chromatographed on silica gel. $Fe_5(CO)_{15}C$ appeared as a gray band which was separated together with any unreacted $Fe_3(CO)_{12}$ from other organo-iron carbonyls by elution with petroleum ether. Mixtures of these two carbonyls are difficult to separate by repeated chromatography or by fractional crystallization. It is therefore necessary that all of the $Fe_3(CO)_{12}$ reacts. The petroleum ether eluate containing $Fe_5(CO)_{15}C$ was concentrated to about 20 ml. yielding about 0.14 g. of the new carbonyl in the most favorable cases. Recrystallization from cyclohexane in a CO-atmosphere yielded black needles or plates which decompose at 110–120° without melting and are partially destroyed during sublimation (50°/0.1 mm.).

Anal. Calcd. for $C_{16}Fe_5O_{15}$: C, 27.01; Fe, 39.25; O, 33.74. Calcd. for $C_{15}Fe_5O_{15}$: C, 25.76; Fe, 39.92; O, 34.32. Found: C, 27.05; Fe, 39.21; O, 33.80.

$Fe_5(CO)_{15}C$ is fairly soluble in petroleum ether and readily so in warm benzene or cyclohexane to give a reddish-gray solution ($\lambda_{max} = 530\ m\mu$, $\epsilon = 353$); it reacts with methylene chloride. In solution it is slowly decomposed by the action of air. It is diamagnetic with $\chi_{mole}^{293°K.} = (-150.4 \pm 3.0) \times 10^{-6}$ cm.^{3}/mole. The infrared spectrum of $Fe_5(CO)_{15}C$ in cyclohexane shows no absorption bands characteristic of bridging carbonyl groups. There are four strong absorption bands at 2049, 2033, 2012, and 1992 cm.$^{-1}$ due to terminal carbonyl groups and one very weak band at 2101 cm.$^{-1}$. Two bands at about 790 and 770 cm.$^{-1}$ may be attributed to Fe-carbide frequencies.

X-Ray Data.—A small needle crystal of dimensions 0.7 × 0.10 × 0.07 mm. was used to obtain the X-ray data. The lattice lengths were determined from precession photographs; the angle β was determined from a Weissenberg photograph.

Multiple-film equi-inclination Weissenberg data were taken for nine reciprocal layers, $h0l$ to $h8l$, with Mo Kα radiation. The intensities of 1165 observed reflections were estimated visually by comparison with a calibrated set of intensities. No absorption corrections were made. Precession data were utilized to correlate the intensities of the Weissenberg data.

Structural Determination Unit Cell and Space Group.—The crystals are monoclinic with lattice parameters a = 16.73 ± 0.03 Å., b = 8.99 ± 0.02 Å., c = 30.38 ± 0.05 Å. and β = 106.9° ± 0.3°; $\rho_{obsd.} = 2.10$ g./cc. *vs.* $\rho_{calcd.} = 2.16$ g./cc. for eight $Fe_5(CO)_{15}C$ species per unit cell. Systematic absences, $h + k$ odd for $\{hkl\}$ and l odd for $\{h0l\}$, indicate either C2/c or Cc as the probable space group; the choice of C2/c was confirmed by the success of the structural determination. All atoms are in the general 8-fold set of positions (8f): $(0,0,0;\ ^1/_2,^1/_2,0) \pm (x,y,z;\ \bar{x},y,^1/_2 - z)$.[11]

Atomic Parameters and Accuracy.—A three-dimensional unsharpened Patterson function was computed. Interpretation of the resultant vector map showed the iron atoms to be in an approximate tetragonal pyramidal configuration. A three-dimensional Fourier synthesis, based on the phases calculated from the iron atoms only, clearly revealed the positions of the fifteen carbonyls in the asymmetric unit. An additional peak appeared in the center of the square formed by the four basal iron atoms. This was interpreted as a carbon atom and refined as such by least squares.

Positional parameters and individual thermal parameters were refined on an IBM 704 computer with a full matrix least-squares program.[12] Standard errors were assigned to the observed structure factors according to the functions $\sigma = 0.1 \times F_0$ if $F_0 > 4F_{min}$ and $\sigma = 0.1 \times 4F_{min}$ if $F_0 \leq 4F_{min}$. For iron the atomic scattering factors used were those of Thomas and Umeda[13]; for carbon and oxygen, the values used were those of Berghuis, *et al.*[14] Four least squares cycles gave successive values of $R_1 = \Sigma||F_0| - |F_c||/\Sigma|F_0|$ of 0.127, 0.085, 0.083, and 0.080.[15] Table I gives the final positional and thermal parameters and their standard deviations. Average standard deviations of atomic positions are 0.004 Å. for iron atoms, 0.037 Å. for carbon atoms, and 0.029 Å. for oxygen atoms.

The phases obtained from the final least-squares refinement were used for computing a three-dimensional electron-density map. A composite [010] projection of the carbon and oxygen peaks from this map is shown in Fig. 1. A three-dimensional difference map showed no peaks of height greater than 1.2 electrons/Å.^{3} No abnormalities appeared in the regions of the iron atoms and the central carbon atom. Comparison of the electron-density distribution of C_{16} on the final Fourier (Fig. 1) with the density distribution of the carbonyl peaks confirmed the identification of C_{16} as a carbon atom. Its individual isotropic temperature factor, 3.5 Å.^{2}, obtained from the final least-squares cycle, is somewhat smaller than the mean value of 4.4 Å.^{2} for the fifteen carbonyl carbons. This lower value is expected, since presumably C_{16} is more tightly bound to the iron atoms than are the carbonyl carbon atoms.

Bond distances and angles with their standard deviations[16] are given in Tables II and III.

Discussion

Description of the Structure.—Crystalline $Fe_5(CO)_{15}C$ consists of discrete, pentameric molecules (Fig. 2) in which the iron atoms are at the corners of a square pyramid. If a small symmetrical distor-

---

[11] "International Tables for X-Ray Crystallography," Vol. I, The Kynoch Press, Birmingham, England, 1952, p. 101.

[12] W. R. Busing and H. A. Levy, "A Crystallographic Least-Squares Refinement Program for the IBM 704," OR XLS, 1959.

[13] L. H. Thomas and K. Umeda, *J. Chem. Phys.*, **26**, 293 (1957).

[14] J. Berghuis, I. M. Haanappel, M. Potters, B. O. Loopstra, C. H. MacGillavry and A. L. Veenendaal, *Acta Cryst.*, **8**, 478 (1955).

[15] Calculated and observed structure factors are deposited as Document 7257 with the American Documentation Institute, Auxiliary Publication Project, Photo Duplication Service, Library of Congress, Washington 25, D. C. A copy may be secured by citing the Document number and by remitting $1.25 for photoprints, or $1.25 for 35 mm. microfilm in advance, by check or money order payable to: Chief, Photoduplication Service, Library of Congress.

[16] W. R. Busing and H. A. Levy, "A Crystallographic Function and Error Program for the IBM 704," OR XFE (1959).

TABLE I

ATOMIC PARAMETERS

Atom	x	y	z	$10^2\ \sigma_x$	$10^2\ \sigma_y$	$10^2\ \sigma_z$	B (Å.^{2})
Fe_1	0.1265	0.3372	0.0856	0.03	0.04	0.01	2.47 ± 0.09
Fe_2	.1668	.0537	.1030	.03	.04	.01	2.69 ± .10
Fe_3	.0406	.1783	.1264	.02	.04	.01	2.61 ± .10
Fe_4	.1438	.3799	.1747	.03	.05	.01	2.68 ± .10
Fe_5	.2674	.2730	.1460	.02	.04	.01	2.60 ± .10
C_1	.1446	.2607	.0369	.22	.45	.14	5.17 ± .80
O_1	.1565	.2264	.0029	.17	.35	.10	6.36 ± .64
C_2	.0183	.3840	.0574	.24	.44	.13	4.94 ± .78
O_2	− .0433	.4276	.0353	.19	.37	.10	7.03 ± .68
C_3	.1660	.5112	.0793	.24	.48	.14	5.48 ± .87
O_3	.1898	.6275	.0723	.19	.44	.11	8.25 ± .79
C_4	.2297	− .0114	.0721	.20	.36	.11	3.83 ± .66
O_4	.2708	− .0657	.0476	.16	.35	.09	6.56 ± .65
C_5	.0854	− .0540	.0683	.22	.44	.12	4.84 ± .75
O_5	.0358	− .1299	.0441	.16	.33	.09	6.04 ± .60
C_6	.2018	− .0748	.1465	.21	.41	.12	4.44 ± .72
O_6	.2264	− .1644	.1765	.16	.35	.10	6.29 ± .61
C_7	.0374	.0465	.1687	.18	.35	.10	3.28 ± .59
O_7	.0328	− .0492	.1949	.15	.33	.09	5.86 ± .57
C_8	− .0432	.1057	.0796	.25	.46	.13	5.37 ± .83
O_8	− .1044	.0742	.0516	.17	.33	.10	6.15 ± .61
C_9	− .0276	.2999	.1408	.16	.29	.09	2.23 ± .50
O_9	− .0800	.3816	.1472	.14	.27	.08	4.65 ± .49
C_{10}	.1134	.3202	.2221	.20	.42	.12	4.22 ± .67
O_{10}	.0919	.2788	.2531	.15	.29	.09	5.28 ± .54
C_{11}	.2296	.4768	.2136	.21	.39	.12	4.25 ± .71
O_{11}	.2812	.5304	.2415	.15	.30	.09	5.24 ± .54
C_{12}	.0857	.5428	.1593	.19	.39	.11	3.85 ± .64
O_{12}	.0524	.6603	.1507	.17	.35	.10	6.42 ± .62
C_{13}	.3288	.2141	.1132	.22	.42	.13	4.95 ± .79
O_{13}	.3799	.1942	.0921	.16	.33	.09	6.01 ± .59
C_{14}	.3328	.1964	.1959	.21	.42	.13	4.52 ± .72
O_{14}	.3805	.1455	.2298	.16	.31	.09	5.85 ± .58
C_{15}	.3140	.4506	.1537	.20	.40	.11	4.15 ± .66
O_{15}	.3458	.5641	.1538	.16	.35	.09	6.22 ± .61
C_{16}	.1565	.2119	.1408	.18	.34	.11	3.46 ± .60

TABLE II

BOND DISTANCES

Bond	Distance, Å.	Bond	Distance, Å.
Fe_2–Fe_1	2.650 ± 0.006	Fe_5–C_{15}	1.76 ± 0.04
Fe_3–Fe_1	2.587 ± .006	Fe_1–C_{16}	1.96 ± .03
Fe_3–Fe_2	2.667 ± .007	Fe_2–C_{16}	1.87 ± .03
Fe_4–Fe_1	2.666 ± .007	Fe_3–C_{16}	1.89 ± .03
Fe_4–Fe_3	2.636 ± .007	Fe_4–C_{16}	1.88 ± .03
Fe_5–Fe_1	2.600 ± .007	Fe_5–C_{16}	1.90 ± .03
Fe_5–Fe_2	2.675 ± .006	C_1–O_1	1.14 ± .04
Fe_2–Fe_4	2.652 ± .007	C_2–O_2	1.13 ± .04
Fe_1–C_1	1.73 ± 0.04	C_3–O_3	1.16 ± .05
Fe_1–C_2	1.82 ± .04	C_4–O_4	1.24 ± .04
Fe_1–C_3	1.73 ± .04	C_5–O_5	1.16 ± .04
Fe_2–C_4	1.70 ± .04	C_6–O_6	1.20 ± .04
Fe_2–C_5	1.76 ± .04	C_7–O_7	1.19 ± .04
Fe_2–C_6	1.73 ± .04	C_8–O_8	1.17 ± .04
Fe_3–C_7	1.76 ± .03	C_9–O_9	1.20 ± .03
Fe_3–C_8	1.82 ± .04	C_{10}–O_{10}	1.16 ± .04
Fe_3–C_9	1.72 ± .03	C_{11}–O_{11}	1.14 ± .03
Fe_4–C_{10}	1.74 ± .04	C_{12}–O_{12}	1.19 ± .04
Fe_4–C_{11}	1.81 ± .04	C_{13}–O_{13}	1.21 ± .04
Fe_4–C_{12}	1.75 ± .04	C_{14}–O_{14}	1.20 ± .04
Fe_5–C_{13}	1.70 ± .04	C_{15}–O_{15}	1.15 ± .04
Fe_5–C_{14}	1.74 ± .04		

tion is neglected, the square pyramid is equilateral; the average Fe–Fe distance is 2.64 Å. Three terminal carbonyls are attached to each iron. The average Fe–C distance of 1.75 Å. is considerably

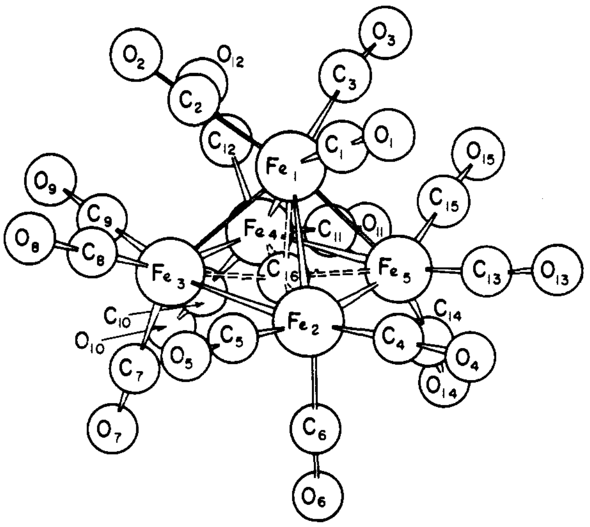

Fig. 2.—Molecular configuration of $Fe_5(CO)_{15}C$.

Table III

Bond Angles

Angle	Degrees	Angle	Degrees
Fe$_1$–Fe$_2$–Fe$_3$	58.2 ± 0.2	Fe$_1$–C$_{16}$–Fe$_3$	84.5 ± 1.2
Fe$_2$–Fe$_1$–Fe$_3$	61.2 ± .2	Fe$_1$–C$_{16}$–Fe$_4$	88.0 ± 1.3
Fe$_2$–Fe$_3$–Fe$_1$	60.6 ± .2	Fe$_1$–C$_{16}$–Fe$_5$	84.7 ± 1.3
Fe$_1$–Fe$_2$–Fe$_5$	58.5 ± .2	C$_{16}$–Fe$_1$–Fe$_2$	44.7 ± 0.9
Fe$_2$–Fe$_1$–Fe$_5$	61.2 ± .2	C$_{16}$–Fe$_1$–Fe$_3$	46.6 ± 0.9
Fe$_2$–Fe$_5$–Fe$_1$	60.3 ± .2	C$_{16}$–Fe$_2$–Fe$_1$	47.6 ± 1.0
Fe$_1$–Fe$_5$–Fe$_4$	61.0 ± .2	C$_{16}$–Fe$_2$–Fe$_3$	45.1 ± 0.9
Fe$_5$–Fe$_1$–Fe$_4$	60.4 ± .2	C$_{16}$–Fe$_2$–Fe$_5$	45.2 ± 0.9
Fe$_1$–Fe$_4$–Fe$_5$	58.5 ± .2	C$_{16}$–Fe$_3$–Fe$_1$	49.0 ± 1.0
Fe$_1$–Fe$_4$–Fe$_3$	58.4 ± .2	C$_{16}$–Fe$_3$–Fe$_2$	44.4 ± 1.0
Fe$_4$–Fe$_1$–Fe$_3$	60.2 ± .2	C$_{16}$–Fe$_3$–Fe$_4$	45.3 ± 1.0
Fe$_4$–Fe$_3$–Fe$_1$	61.4 ± .2	C$_{16}$–Fe$_4$–Fe$_1$	47.3 ± 1.0
Fe$_4$–Fe$_1$–Fe$_2$	89.4 ± .2	C$_{16}$–Fe$_4$–Fe$_3$	45.7 ± 0.9
Fe$_3$–Fe$_1$–Fe$_5$	93.2 ± .2	C$_{16}$–Fe$_4$–Fe$_5$	45.8 ± 0.9
Fe$_2$–Fe$_3$–Fe$_4$	89.7 ± .2	C$_{16}$–Fe$_5$–Fe$_1$	48.7 ± 0.9
Fe$_3$–Fe$_4$–Fe$_5$	90.9 ± .2	C$_{16}$–Fe$_5$–Fe$_2$	44.3 ± 1.0
Fe$_4$–Fe$_5$–Fe$_2$	89.2 ± .2	C$_{16}$–Fe$_5$–Fe$_4$	45.0 ± 1.0
Fe$_5$–Fe$_2$–Fe$_3$	89.8 ± .2	C$_{16}$–Fe$_1$–Fe$_4$	44.7 ± 0.9
Fe$_5$–C$_{16}$–Fe$_3$	169.1 ± 1.9	C$_{16}$–Fe$_1$–Fe$_5$	46.7 ± 0.9
Fe$_4$–C$_{16}$–Fe$_2$	175.6 ± 1.9	C$_1$–Fe$_1$–C$_2$	95.2 ± 1.7
Fe$_2$–C$_{16}$–Fe$_3$	90.5 ± 1.3	C$_1$–Fe$_1$–C$_3$	95.6 ± 1.9
Fe$_3$–C$_{16}$–Fe$_4$	88.9 ± 1.3	C$_2$–Fe$_1$–C$_3$	95.8 ± 1.8
Fe$_4$–C$_{16}$–Fe$_5$	89.2 ± 1.3	C$_4$–Fe$_2$–C$_5$	88.7 ± 1.6
Fe$_5$–C$_{16}$–Fe$_2$	90.5 ± 1.4	C$_4$–Fe$_2$–C$_6$	93.8 ± 1.6
Fe$_1$–C$_{16}$–Fe$_2$	87.6 ± 1.3	C$_5$–Fe$_2$–C$_6$	97.0 ± 1.7
C$_7$–Fe$_3$–C$_8$	98.6 ± 1.6	C$_{16}$–Fe$_1$–C$_1$	115.8 ± 1.6
C$_7$–Fe$_3$–C$_9$	94.5 ± 1.3	C$_{16}$–Fe$_1$–C$_2$	120.6 ± 1.5
C$_8$–Fe$_3$–C$_9$	90.5 ± 1.5	C$_{16}$–Fe$_1$–C$_3$	127.0 ± 1.6
C$_{10}$–Fe$_4$–C$_{11}$	88.7 ± 1.6	C$_1$–Fe$_1$–Fe$_2$	72.0 ± 1.3
C$_{10}$–Fe$_4$–C$_{12}$	101.8 ± 1.6	C$_2$–Fe$_1$–Fe$_3$	74.6 ± 1.2
C$_{11}$–Fe$_4$–C$_{12}$	92.7 ± 1.5	C$_1$–Fe$_1$–Fe$_5$	99.5 ± 1.2
C$_{13}$–Fe$_5$–C$_{14}$	93.0 ± 1.7	C$_2$–Fe$_1$–Fe$_4$	104.1 ± 1.2
C$_{13}$–Fe$_5$–C$_{15}$	92.2 ± 1.7	C$_1$–Fe$_1$–Fe$_3$	116.7 ± 1.3
C$_{14}$–Fe$_5$–C$_{15}$	95.9 ± 1.6	C$_2$–Fe$_1$–Fe$_2$	118.6 ± 1.3
O$_1$–C$_1$–Fe$_1$	172.2 ± 3.6	C$_1$–Fe$_1$–Fe$_4$	158.1 ± 1.3
O$_2$–C$_2$–Fe$_1$	168.2 ± 3.5	C$_2$–Fe$_1$–Fe$_5$	164.2 ± 1.2
O$_3$–C$_3$–Fe$_1$	175.9 ± 3.9	C$_3$–Fe$_1$–Fe$_2$	143.9 ± 1.3
O$_4$–C$_4$–Fe$_2$	175.3 ± 2.7	C$_3$–Fe$_1$–Fe$_3$	146.7 ± 1.4
O$_5$–C$_5$–Fe$_2$	175.0 ± 3.3	C$_3$–Fe$_1$–Fe$_4$	92.8 ± 1.4
O$_6$–C$_6$–Fe$_2$	179.5 ± 3.3	C$_3$–Fe$_1$–Fe$_5$	88.9 ± 1.3
O$_7$–C$_7$–Fe$_3$	175.5 ± 2.8	C$_{16}$–Fe$_2$–C$_4$	141.5 ± 1.5
O$_8$–C$_8$–Fe$_3$	169.7 ± 3.4	C$_{16}$–Fe$_2$–C$_5$	126.5 ± 1.5
O$_9$–C$_9$–Fe$_3$	174.3 ± 2.4	C$_{16}$–Fe$_2$–C$_6$	96.4 ± 1.5
O$_{10}$–C$_{10}$–Fe$_4$	178.6 ± 3.0	C$_4$–Fe$_2$–Fe$_4$	140.8 ± 1.1
O$_{11}$–C$_{11}$–Fe$_4$	172.9 ± 3.2	C$_5$–Fe$_2$–Fe$_4$	126.1 ± 1.2
O$_{12}$–C$_{12}$–Fe$_4$	174.3 ± 2.9	C$_4$–Fe$_2$–Fe$_3$	162.9 ± 1.1
O$_{13}$–C$_{13}$–Fe$_5$	169.0 ± 3.2	C$_5$–Fe$_2$–Fe$_5$	166.1 ± 1.2
O$_{14}$–C$_{14}$–Fe$_5$	177.4 ± 3.2	C$_4$–Fe$_2$–Fe$_1$	112.5 ± 1.1
O$_{15}$–C$_{15}$–Fe$_5$	172.3 ± 3.2	C$_5$–Fe$_2$–Fe$_1$	107.6 ± 1.2
C$_5$–Fe$_2$–Fe$_3$	81.6 ± 1.2	C$_4$–Fe$_2$–Fe$_5$	96.8 ± 1.1
C$_6$–Fe$_2$–Fe$_1$	143.8 ± 1.2	C$_{12}$–Fe$_4$–Fe$_5$	130.1 ± 1.1
C$_6$–Fe$_2$–Fe$_3$	101.3 ± 1.2	C$_{11}$–Fe$_4$–Fe$_3$	165.5 ± 1.1
C$_6$–Fe$_2$–Fe$_4$	98.6 ± 1.2	C$_{12}$–Fe$_4$–Fe$_1$	87.8 ± 1.1
C$_6$–Fe$_2$–Fe$_5$	95.4 ± 1.2	C$_{11}$–Fe$_4$–Fe$_1$	124.5 ± 1.1
C$_{16}$–Fe$_3$–C$_8$	138.7 ± 1.6	C$_{12}$–Fe$_4$–Fe$_3$	101.7 ± 1.1
C$_{16}$–Fe$_3$–C$_9$	123.5 ± 1.3	C$_{11}$–Fe$_4$–Fe$_5$	80.8 ± 1.1
C$_{16}$–Fe$_3$–C$_7$	100.8 ± 1.3	C$_{10}$–Fe$_4$–Fe$_1$	145.3 ± 1.2
C$_8$–Fe$_3$–Fe$_5$	136.3 ± 1.2	C$_{10}$–Fe$_4$–Fe$_5$	127.1 ± 1.1
C$_9$–Fe$_3$–Fe$_5$	121.9 ± 0.9	C$_{10}$–Fe$_4$–Fe$_2$	110.1 ± 1.2
C$_8$–Fe$_3$–Fe$_4$	157.0 ± 1.3	C$_{10}$–Fe$_4$–Fe$_3$	86.9 ± 1.1
C$_9$–Fe$_3$–Fe$_2$	165.5 ± 0.9	C$_{16}$–Fe$_5$–C$_{15}$	131.1 ± 1.4
C$_8$–Fe$_3$–Fe$_1$	103.5 ± 1.3	C$_{16}$–Fe$_5$–C$_{13}$	126.9 ± 1.6
C$_9$–Fe$_3$–Fe$_1$	105.9 ± 0.9	C$_{16}$–Fe$_5$–C$_{14}$	108.2 ± 1.5
C$_8$–Fe$_3$–Fe$_2$	97.6 ± 1.3	C$_{15}$–Fe$_5$–Fe$_3$	127.8 ± 1.1
C$_9$–Fe$_3$–Fe$_4$	78.4 ± 0.9	C$_{13}$–Fe$_5$–Fe$_3$	126.0 ± 1.2
C$_7$–Fe$_3$–Fe$_1$	149.5 ± 1.0	C$_{15}$–Fe$_5$–Fe$_2$	157.5 ± 1.1
C$_7$–Fe$_3$–Fe$_5$	106.3 ± 0.9	C$_{13}$–Fe$_5$–Fe$_4$	164.4 ± 1.2
C$_7$–Fe$_3$–Fe$_4$	102.2 ± 1.0	C$_{15}$–Fe$_5$–Fe$_1$	99.7 ± 1.1
C$_7$–Fe$_3$–Fe$_2$	96.2 ± 1.0	C$_{13}$–Fe$_5$–Fe$_1$	103.5 ± 1.2
C$_{16}$–Fe$_4$–C$_{12}$	132.2 ± 1.4	C$_{15}$–Fe$_5$–Fe$_4$	89.3 ± 1.1
C$_{16}$–Fe$_4$–C$_{11}$	123.6 ± 1.4	C$_{13}$–Fe$_5$–Fe$_2$	83.5 ± 1.2
C$_{16}$–Fe$_4$–C$_{10}$	108.3 ± 1.6	C$_{14}$–Fe$_5$–Fe$_1$	156.7 ± 1.2
C$_{12}$–Fe$_4$–Fe$_2$	130.2 ± 1.1	C$_{14}$–Fe$_5$–Fe$_3$	113.5 ± 1.2
C$_{11}$–Fe$_4$–Fe$_2$	124.4 ± 1.1	C$_{14}$–Fe$_5$–Fe$_2$	106.4 ± 1.2
		C$_{14}$–Fe$_5$–Fe$_4$	102.2 ± 1.2

shorter than the sum of the single bond covalent radii which is 1.95 Å.; the average C–O separation of 1.17 Å. agrees well with that in other metal carbonyls. The [010] projection of the unit cell (Fig. 3) indicates the packing of the molecules. The O· · ·O contact distances between molecules range from 2.9 to 3.9 Å.

As with other polynuclear metal carbonyls[17] the feature determining the structure is the ability of each iron atom to form the inert gas shell of electrons by both metal–metal and metal-carbonyl bonding. In $Fe_5(CO)_{15}C$, however, the inert gas configuration is achieved in a remarkable, new way by additional bonding of the iron atoms to a carbide atom. The carbide atom, C_{16}, is located slightly below the center of the basal plane of iron atoms and is at an average distance of 1.89 Å. from the four basal iron atoms and at a distance of 1.96 Å. from the apical iron atom. It is probable that the carbide atom in $Fe_5(CO)_{15}C$ originates by reduction of carbon monoxide.

The existence of the carbide atom with four valence electrons available for bonding allows the pairing-up of the unpaired electron on each of the four basal irons and enables them to obtain the "krypton" configuration. Of course, this bookkeeping of electrons says nothing about the electron charge distribution that results when the carbon atom coördinates with the *five* iron atoms.

Although a pentamer is the only species which obeys the Sidgwick rule[18] for a 1:3 ratio of Fe:CO groups, this rule contains the inherent assumption of metal–metal bonding from each metal to every other metal. The diagonal Fe–Fe distances across the basal plane, 3.75 Å., are too great for a pairing of electrons. The important feature of the carbide atom in $Fe_5(CO)_{15}C$ is that its presence enables this difficulty to be overcome. Without this atom the square pyramidal molecular configuration could not conform to the inert gas configuration unless unusual multi-centered metal–metal bonding were invoked. Hence, both metal–metal bonds and metal–carbon bonds cooperate to determine the resulting structure.

(17) (a) H. M. Powell and R. V. G. Ewens, *J. Chem. Soc.*, 286 (1939). (b) L. F. Dahl and R. E. Rundle, *J. Chem. Phys.*, **26**, 1751 (1957). (c) L. F. Dahl, E. Ishishi and R. E. Rundle, *ibid.*, **26**, 1750 (1957). (d) P. Corradini, *ibid.*, **31**, 1676 (1959). (e) G. G. Summer and H. P. Klug, Abstracts of Papers, National Meeting of the American Crystallographic Association, Boulder, Colorado, July–August 1960. (f) E. R. Corey and L. F. Dahl, *J. Am Chem. Soc.*, **83**, 2203 (1961); E. R. Corey and L. F. Dahl, *Inorg. Chem.*, **1**, 521 (1962).

(18) N. V. Sidgwick and R. W. Bailey, *Proc. Roy. Soc. (London)*, **144**, 521 (1934).

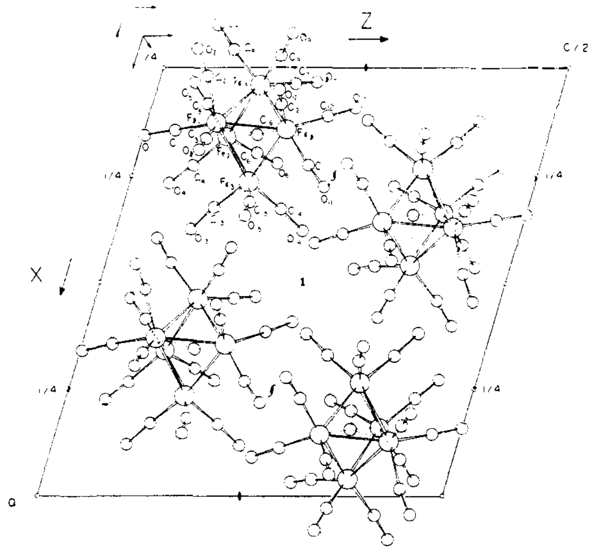

Fig. 3.—[010] projection of the unit cell.

Discussion of Infrared Spectrum.—The structure with three terminal carbonyl groups on each metal is in accord with the observed infrared spectrum which shows no absorption bands in the 1800 cm.$^{-1}$ region characteristic of symmetrical carbonyl bridges. An interpretation of part of the observed infrared spectrum can be made with the assumption that the coupling between the different tricarbonyl fragments can be neglected, and that only the local C_{3v} symmetry of the carbonyl groups need be considered.[19] Each iron tricarbonyl fragment would give rise to two infrared active C–O stretching fundamentals of symmetry A_1 and E. Since the molecular structure has two kinds of iron tricarbonyl fragments, apical and basal, two pairs of bands would be predicted; and indeed four bands are observed in the 2000 cm.$^{-1}$ region. Alternatively, it is possible that the difference between the geometrically dissimilar apical and basal tricarbonyl fragments may be too small to cause an observable shift in carbonyl frequency; in this case two of the observed bands must be rationalized as the fundamentals and the other two as overtone or combination bands.

Discussion of Bonding.—To gain better insight into the bonding of the carbide to the five iron atoms, a qualitative l.c.a.o.–m.o. treatment will be outlined for the molecule. In order to make the m.o. treatment tractable, the molecular symmetry will be idealized (Fig. 4) as described below. A Cartesian molecular coördinate system is chosen with the x and y axes parallel to the two diagonals of the square formed by the basal iron atoms, and with the z axis perpendicular to the resulting plane of basal iron atoms. The apical iron will be assumed to possess C_{3v} local symmetry in the interaction of its orbitals with the three carbonyls attached to it and C_{4v} symmetry in its interaction with the rest of the molecule. For simplicity the metal–carbonyl double bonding is neglected. The C_{4v} transformation scheme for the basal and apical iron orbitals

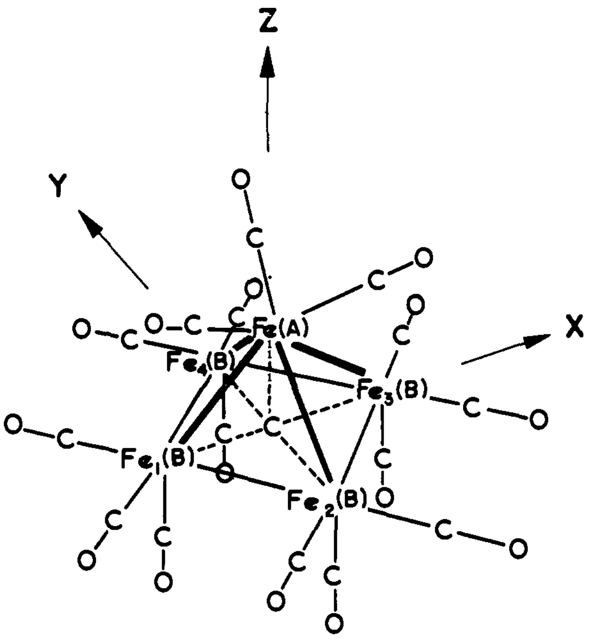

Fig. 4.—Idealized molecular configuration of $Fe_5(CO)_{14}C$. The iron atoms are located at the corners of a square pyramid. The $Fe_4(CO)_{12}C$ fragment is of C_{4v} symmetry; the apical $Fe(CO)_3$ fragment is of C_{3v} symmetry. The local environment about each basal iron is octahedral.

which can be utilized for bonding with the carbide orbitals is given in Table IV.

Consider first the available orbitals of the four basal iron atoms. Each iron is assumed to possess an octahedral environment such that five octahedral-type hybrid orbitals formed from the d_{xy}, d_{z^2}, s, $1/\sqrt{2}\ (p_x + p_y)$, $1/\sqrt{2}\ (p_x - p_y)$, and p_z a.o.'s are utilized in σ-bonding to the three bonded carbonyls and to the two neighboring basal iron atoms. The 6th octahedral orbital of each of these four irons is then directed along the Z axis[20]; linear combination of these four octahedral orbitals (denoted by o_n) give four symmetry orbitals which are classified according to the irreducible representations of C_{4v} (Table IV).

Certain SO combinations also are given in Table IV for the $d_{x^2-y^2}$, d_{xz}, and d_{yz} basal iron orbitals. The major contribution to the multi-centered delocalized σ-type bonding of the basal irons to the carbide results from the efficient overlap of the $d_{x^2-y^2}$ SO's of a_1 and e symmetry with the $s'(a_1)$, p_x' (e_x), and p_y' (e_y) carbide orbitals. The (d_{xz}, d_{yz}) SO combinations for the basal irons can overlap with the apical iron orbitals of the same symmetry; furthermore, a $d\pi$–$p\pi$ type interaction of the a_1 (d_{xz}, d_{yz}) SO combination with the p_z' carbide orbital is possible. Although these interactions involving the (d_{xz}, d_{yz}) SO's would need to be considered

---

[19] The assumption of C_{3v} symmetry for each of the basal iron tricarbonyls actually is not valid due to the considerable distortion of the carbonyl groups but is ignored for these rationalizations.

[20] The structural determination shows that the carbonyl groups attached to the basal iron atoms are positioned such that the idealized octahedron about the basal iron atom does not have its coördinate axes coincident with the molecular axes, and the octahedral-type orbitals are directed more nearly toward the apical iron. The orbitals for each basal iron can be referred to a localized atomic coördinate system still satisfying C_{4v} symmetry but rotated to allow for the observed distortion. Since this distortion does not affect the symmetry classifications, it will be neglected.

TABLE IV

ORBITAL TRANSFORMATION SCHEME IN C_{4v} SYMMETRY FOR INTERACTION OF FIVE IRON ATOMS WITH CARBIDE ATOM

Irreducible representation	Basal iron SO's (Fe_4)	Carbide orbitals	Apical iron orbitals
a_1	$^1/_2(o_1 + o_2 + o_3 + o_4)$	p_z'	$a_1s'' + a_2d_{z^2}'' - a_3p_z''$
	$^1/_2(d_{xz(1)} + d_{yz(2)} + d_{xz(3)} + d_{yz(4)})$		
	$^1/_2(d_{x^2-y^2(1)} - d_{x^2-y^2(2)} + d_{x^2-y^2(3)} - d_{x^2-y^2(4)})$	s'	
			$a_4s'' - a_5d_{z^2}''$
e_x	$1/\sqrt{2}(o_3 - o_1)$		$b_1p_x'' - b_2d_{xz}''$
	$1/\sqrt{2}(d_{xz(3)} - d_{xz(1)})$		
	$1/\sqrt{2}(d_{x^2-y^2(3)} - d_{x^2-y^2(1)})$	p_x'	
e_y	$1/\sqrt{2}(o_4 - o_2)$		$b_1p_y'' - b_2d_{yz}''$
	$1/\sqrt{2}(d_{yz(4)} - d_{yz(2)})$		
	$1/\sqrt{2}(d_{x^2-y^2(4)} - d_{x^2-y^2(2)})$	p_y'	
b_1	$^1/_2(o_1 - o_2 + o_3 - o_4)$		$d_{x^2-y^2}''$
	$^1/_2(d_{xz(1)} - d_{yz(2)} + d_{xz(3)} - d_{yz(4)})$		
	$^1/_2(d_{x^2-y^2(1)} + d_{x^2-y^2(2)} + d_{x^2-y^2(3)} + d_{x^2-y^2(4)})$		
b_2			d_{xy}''

in the detailed calculation of the energetics of the molecule, for purposes of visualizing the bonding these interactions are ignored. The overlap of the a_1 $d_{x^2-y^2}$ basal iron SO with the carbide p_z' (a_1) orbital and the (d_{xz}, d_{yz}) SO's with the s', p_x', and p_y' orbitals of the same irreducible representation is relatively small[21] and can be ignored.

Consider the bonding of the apical iron. Three apical iron hybrid orbitals of a_1 symmetry and two pairs of e symmetry can be readily obtained. Since the localized environment about the apical iron is not symmetrical, these hybrid orbitals are not equivalent; different weighting coefficients, a_i and b_i, are used for the different hybrid combinations. Within the framework of simple l.c.a.o.-m.o. theory these coefficients in principle can be varied to make the bond energies a maximum and the molecular energy a minimum. One a_1 hybrid orbital of form $a_6s'' + a_7d_{z^2}'' + a_8p_z''$ and one pair of e symmetry, $b_3p_x'' + b_4d_{xz}''$ and $b_3p_y'' + b_4d_{yz}''$, can be used for σ-bonding to the three carbonyl groups. The important interactions of the apical iron with the Fe_4C fragment involve the overlap of the axially symmetric hybrid orbital, $a_1s'' + a_2d_{z^2}'' - a_3p_z''$, of a_1 symmetry and the pair of hybrid orbitals, $b_1p_x'' - b_2d_{xz}''$ and $b_1p_y'' - b_2d_{yz}''$, of e symmetry with the orbitals of equivalent symmetry belonging to the Fe_4C fragment. The hybrid orbital $a_4s'' - a_5d_{z^2}''(a_1)$ and the $d_{x^2-y^2}''$ (b_1) orbital, both of which are maximized in the xy-plane containing the apical iron, overlap to a lesser extent; the d_{xy}'' (b_2) orbital is by symmetry non-bonding to the Fe_4C fragment. The above representation of bonding for the apical iron is formally analogous to that for cyclobutadiene-iron tricarbonyl[22] except that for $Fe_5(CO)_{15}C$ the carbide atom introduces 6-centered m.o.'s.

This representation of the bonding shows the possible interactions of the carbide atom with all five iron atoms. Such interactions would lead to a fractional bond order for the bonding of the carbon to the five iron atoms.

The delocalized bonding of the carbide atom to the five irons in $Fe_5(CO)_{15}C$ is related no doubt to the Fe–C bonding in Fe_3C in which the carbon atoms are in the interstices of nearly regular trigonal pyramidal prisms of iron atoms.[23] The four valence orbitals of the carbide atom must be utilized in bonding to six iron atoms. It must be emphasized that the carbide atom in $Fe_5(CO)_{15}C$ is pentacoördinated whereas the carbide atoms in Fe_3C and other so-called interstitial carbide compounds are invariably hexacoördinated. The Fe–C distances in Fe_3C vary from 1.85 to 2.01 Å. and the Fe–Fe distances from 2.49 to 2.68 Å.[23]

Bond lengths reported for localized (*i.e.*, normal electron-pair interactions) Fe–C σ-bonds are 1.95 Å. (av.) for $Fe_2(CO)_6(COH)_2(CH_3C_2CH_3)$,[24] 2.01–2.10 Å. for $Fe_2(CO)_6(C_6H_5C_2H)_3$,[25] and 2.11–2.18 Å. for several conjugated diene–iron complexes[26] which interact *via* two σ-bonds to the terminal carbons and a "bent" μ-type bond to the central olefinic group.[26c] At present, no simple explanation can be given for the large variance of these observed values.

Of interest is the comparison of the average Fe–Fe distance of 2.64 Å. in $Fe_5(CO)_{15}C$ with Fe–Fe distances in other carbonyl compounds with metal–metal bonds. Shorter Fe–Fe distances are found in $Fe_2(CO)_9$ (2.46 Å.),[17a] $(C_5H_5)_2Fe_2(CO)_4$ (2.49 Å.),[27] $Fe_2(CO)_6(COH)_2(CH_3C_2CH_3)$ (2.49 Å.),[24] $Fe_2(CO)_6(C_6H_5C_2H)_3$ (2.50 Å.),[25] the black isomer of $Fe_3(CO)_8(C_6H_5C_2C_6H_5)_2$ (2.43 Å. (av.)),[28] and the violet isomer of $Fe_3(CO)_8(C_6H_5C_2C_6H_5)_2$ (2.46 Å.(av.) and

---

(21) The orbitals are orthogonal for the carbide atom in the plane of the basal iron atoms.

(22) For reference to bonding in cyclobutadiene–metal complexes see: (a) H. C. Longuet-Higgins and L. E. Orgel, *J. Chem. Soc.*, 1969 (1956). (b) D. A. Brown, *J. Inorg. Nuclear Chem.*, **10**, 39 and 49 (1959). (c) G. E. Coates, "Organometallic Compounds," J. Wiley and Sons, Inc., New York, N. Y., 1961, pp. 329–331.

(23) R. W. G. Wyckoff, "Crystal Structures," Vol. II, Interscience Publishers, Inc., New York, N. Y., p. 24.

(24) A. A. Hock and O. S. Mills, *Proc. Chem. Soc.* (*London*), 233 (1958); *Acta Cryst.*, **14**, 139 (1962).

(25) G. S. D. King, *ibid.*, **15**, 243 (1962).

(26) (a) O. S. Mills and G. Robinson, *Proc. Chem. Soc.* (*London*), 421 (1960). (b) B. Dickens and W. N. Lipscomb, *J. Am. Chem. Soc.*, **83**, 489 and 4862 (1961). (c) D. L. Smith and L. F. Dahl, *ibid.*, **84**, 1743 (1962). (d) R. P. Dodge and V. Schomaker, private communication, 1961.

(27) O. S. Mills, *Acta Cryst.*, **11**, 620 (1958).

(28) R. P. Dodge and V. Schomaker, private communication, 1960; abstracts of papers, National Meeting of the American Crystallographic Association, Villanova University, June, 1962.

2.59 Å.);[28] longer Fe–Fe distances are observed in Fe$_3$(CO)$_{12}$ (*ca.* 2.75 Å.),[17b] and Fe$_2$(CO)$_8^{2-}$ (2.88 Å.).[29] The variation of iron–iron distances can be rationalized in terms of the amount of negative charge localized on the metal atom through coördination with the other ligands. In general, greater metal–metal distances correspond to a higher localized negative charge.

Acknowledgments.—The authors are grateful to Mr. G. S. D. King of Union Carbide European Research Associates and Mr. Paul Sutton of Wisconsin for helpful discussions. The X-ray work was financially supported by the National Science Foundation (Grant No. 86-3474).

(29) O. S. Mills, private communication, 1961; R. S. Nyholm, *Proc. Chem. Soc. (London)*, 273 (1961).

[CONTRIBUTION FROM THE DEPARTMENT OF CHEMISTRY AND RESEARCH LABORATORY OF ELECTRONICS, MASSACHUSETTS INSTITUTE OF TECHNOLOGY, CAMBRIDGE, MASSACHUSETTS]

Relaxation Spectra of Some Nickel(II) and Cobalt(II) Complexes[1]

BY GORDON G. HAMMES AND JEFFREY I. STEINFELD

RECEIVED JULY 9, 1962

The rate constants for the formation and dissociation of Ni(II) and Co(II) complexes with one, two and three glycine, diglycine, or imidazole molecules have been determined by the temperature-jump technique. The approximate time scale of the reactions studied ranged from 0.1 to 500 msec. The rate-determining step of the complex-building reaction, following initial formation of an ion pair, is the dissociation of a water molecule from the inner hydration sphere of the metal ion. The measured rate constants can be normalized with respect to electrostatic and steric factors by dividing out the calculated ion-pair equilibrium constant. The rate constant of dissociation thus obtained is characteristic of a given metal ion, and, in nearly all the reactions studied, was 20 to 25 times greater for Co(II) than for Ni(II). The difference in activation energies corresponding to this rate ratio is of the order of magnitude predicted on the basis of crystal-field theories. For glycine, these normalized rate constants tend to increase in reactions involving the higher complexes, indicating a loosening of the hydration shell due to the fact that the glycine is bound to the metal *via* the negatively charged carboxyl group. These rate constants are independent of the number of ligands bound if the bonding takes place *via* uncharged groups.

Introduction

Although the equilibrium properties of transition metal ion complexes have received considerable attention,[2] relatively few systematic kinetic studies have been carried out on any of these complexes other than those of Co(III) and Pt(II). This is primarily due to the fact that most of the reactions of complexes of other transition metal ions proceed too fast to be studied by conventional techniques. However, the recent application of relaxation methods to simple metal complex systems[3-4] indicates that these new fast reaction techniques are applicable to multi-ligand metal complexes as well.

In the present study, the temperature jump method[5,6] has been used to study the reactions of Ni(II) and Co(II) with glycine, glycylglycine (diglycine) and imidazole. In each case, the metal ions are known to bind several of the ligand molecules and the equilibrium quotients for the individual complex formation steps have been determined.[1,7-10] The rate constants obtained in this study are consistent with the detailed mechanism proposed by Eigen and co-workers for simple systems,[3,4] namely, that the rate of release of water molecules from the inner coördination sphere of the metal ion is the rate controlling step in the overall rate of complex formation. However, this rate of dissociation is greatly dependent on the number and mode of bonding of ligand molecules on the metal. In fact, the variation of this rate constant with successive degrees of association of the ligand with the metal permits some conclusions to be drawn concerning the structure of the complexes.

The metal ions Co(II) and Ni(II) were selected for study because the ratio of their rates of reaction in similar bonding situations is a direct measure of the difference in their crystal field activation energies.[11,12] Moreover, the observed ratios of rate constants can provide a measure of the difference in crystal field stabilization energy in cases where *ab initio* calculations of this quantity are exceedingly difficult.

Finally, relatively simple systems such as those studied can serve as model systems for problems of biochemical interest, such as metal ion activation of enzymes, and the association of metals with proteins and polynucleotides. Kinetic properties, especially at the molecular level, are potentially capable of yielding more specific information than equilibrium properties.

Experimental

The temperature jump apparatus used has been described in considerable detail elsewhere.[13] The only significant change made is that a single beam of light is now employed, rather than a double beam. A null detection method is still made possible by offsetting the initial photomultiplier voltage with a potentiometer powered by dry cells. This

---

(1) This work was supported in part by the U. S. Army Signal Corps, Air Force, Office of Scientific Research, and Office of Naval Research and in part by the National Institutes of Health (RG7803).

(2) See for example J. Bjerrum, G. Schwarzenbach and L. G. Sillén, "Stability Constants of Metal Ion Complexes," Chemical Society, London, 1957.

(3) M. Eigen, *Z. Elektrochem.*, **64**, 115 (1960).

(4) (a) M. Eigen and K. Tamm, *ibid.*, **66**, 93 (1962); (b) M. Eigen and K. Tamm, *ibid.*, **66**, 107 (1962).

(5) G. Czerlinski and M. Eigen, *ibid.*, **63**, 652 (1959).

(6) H. Diebler, Dissertation, Universität Göttingen, 1960.

(7) R. B. Martin, M. Chamberlin and J. T. Edsall, *J. Am. Chem. Soc.*, **82**, 495 (1960).

(8) J. B. Gilbert, M. C. Otey and J. Z. Hearon, *ibid.*, **77**, 2599 (1955).

(9) C. Tanford, D. C. Kirk, Jr., and M. V. Chantooni, Jr., *ibid.*, **76**, 5325 (1954).

(10) R. Mathur and H. Lal, *J. Phys. Chem.*, **63**, 439 (1959).

(11) R. G. Pearson, *ibid.*, **63**, 321 (1959).

(12) F. Basolo and R. G. Pearson, "Mechanisms of Inorganic Reactions," John Wiley and Sons, New York, N. Y., 1958.

(13) G. G. Hammes and P. Fasella, *J. Am. Chem. Soc.*, in preparation.